Base-Catalyzed Hydrogen/Deuterium Exchange between Water and Acetonitrile in Anionic Water Clusters

O. Petru Balaj, Chi-Kit Siu, Iulia Balteanu, Brigitte S. Fox-Beyer, Martin K. Beyer,* and Vladimir E. Bondybey*

Institut für Physikalische und Theoretische Chemie, Technische Universität München, Lichtenbergstrasse 4, 85747 Garching, Germany

Received: May 13, 2004; In Final Form: July 1, 2004

An H/D-exchange reaction involving the methyl group of acetonitrile is observed in the small anionic water cluster $OH^-(CD_3CN)(H_2O)_2$. In this cluster, a randomization of H and D atoms takes place, and in subsequent collisions with CD_3CN, the potentially partially deuterated acetonitrile is replaced by the fully deuterated species. In sequential collisions, fully deuterated clusters $OD^-(CD_3CN)(D_2O)_2$ are obtained as final products. The H/D-exchange does not occur in $OH^-(CD_3CN)(H_2O)_3$ or larger clusters. Density functional calculations show that in these larger species, the OH^- no longer directly attacks the methyl group, and the barriers for H/D-exchange become higher than those for ligand loss reaction channels. This is a very subtle influence of solvation on an H/D-exchange reaction in the gas phase, where a relatively acidic methyl group encounters a strongly basic reaction partner.

Introduction

In mass spectrometric experiments, hydrogen/deuterium exchange reactions are frequently used as a probe of gas-phase structures of peptides and proteins.[1−10] This exchange is specific to acidic or basic sites, and methyl groups are in general considered to be unaffected. However, flowing afterglow studies have shown that certain carbanions undergo efficient H/D-exchange with H_2O.[11,12] CH_2CN^- was shown to sequentially exchange both H atoms against D in collisions with H_2O. In the present manuscript, we describe an example of H/D-exchange involving the methyl group of acetonitrile, which we encountered in experiments with hydrated electrons. The observations are quite puzzling, since in the first place, the methyl group is involved, and second, solvation hinders rather than promotes the exchange.

The energy needed to ionize atoms or molecules is relatively high, and free electrons therefore usually only occur in energy rich environments such as discharges, plasmas, and flames. However, electrons can also be prepared in condensed, liquid, or solid systems[13−17] but are very reactive even when stabilized by solvation. Their chemistry has been extensively studied, most often in pulsed radiolysis experiments, where they are produced by the impact of high energy electron beams in bulk solution.[18] In recent years it has been demonstrated that electrons solvated in finite solvent nanodroplets also can be produced, and the stability, structure, and reactivity of such hydrated electrons have been investigated.[19−25] A laser vaporization source developed in our laboratory turns out to be a very efficient source of $(H_2O)_n^-$ species, which can be trapped and studied by high-resolution FT-ICR mass spectrometry.

The advantage of such clusters, whose sizes are typically in the range $n = 13-80$, is that their masses, and thus their elemental composition, are exactly known, eliminating any effects due to impurities, and also the presence of H_3O^+ ions from the autoprotolysis of water can be ruled out in such clusters of typically less than 100 water molecules. Investigations of the reactions of such aqueous electrons with a number of small inorganic and organic molecules yielded quite a varied and multifaceted chemistry, and recently we have reported a particularly interesting reaction with acetonitrile.[25]

The hydrated electron clusters react very efficiently with acetonitrile, according to the equation:

$$(H_2O)_n^- + CH_3CN \rightarrow OH^-(H_2O)_{n-x-1} + CH_3CHN + xH_2O \quad (1)$$

Although mass spectrometry gives no direct information about either the mechanisms of the reactions which take place or about the structure of the neutral products, it appears very likely that the first step here involves an interaction of acetonitrile with the electron. While the anion of bare acetonitrile is only weakly dipole bound, previous studies[25−28] indicate that solvation stabilizes a covalent CH_3CN^- radical anion. This anion then withdraws a proton from one of the water ligands, forming a neutral CH_3CHN radical, which is only weakly held in the cluster. This radical evaporates from the cluster surface, possibly accompanied by additional water molecules. This process must be faster than 100 ms, since no product clusters containing acetonitrile are observed in the first reaction step.

The purpose of the present work is to investigate the fate of these hydrated hydroxyl clusters and their further reactions upon subsequent collisions with the acetonitrile reactant. With the help of fully deuterated CD_3CN, the conditions and the mechanism for H/D-exchange between the water molecules and the methyl group are elucidated, and the findings are compared with the results of density functional theory calculations.

Experimental Details

The experiments were performed on a modified Bruker/Spectrospin CMS47X FT-ICR mass spectrometer, equipped with an APEX III data station and a home-built laser vaporization

* To whom correspondence should be addressed. E-mail: beyer@ch.tum.de, bondybey@ch.tum.de. Fax: ++49-89-289-13416.

10.1021/jp047955e CCC: $27.50
Published on Web 08/24/2004

source.[29−31] Using this source we are capable to generate and therefore study a large variety of hydrated ions.[23,32] Hydrated electrons $(H_2O)_n^-$, have been generated in the laser vaporization cluster source as described previously.[24,25] In this source, a rotating zinc target is vaporized by a pulsed, frequency doubled Nd:YAG laser beam in the presence of a high pressure carrier gas pulse, which consists of helium seeded with small amounts of water vapor. The hot plasma produced by the vaporization is rapidly cooled by dilution with the cold carrier gas, which is supplied via a home-built pulsed piezoelectric valve. Upon further cooling by supersonic expansion into high vacuum, clusters and complexes are formed. To avoid the production of metal anions, zinc with its closed $3d^{10}4s^2$ valence shell and positive electron affinity, was used in the present work as target material. The hydrated electron clusters are then guided from the source through several stages of differential pumping along the field axis of a 4.7 T superconducting magnet and into the ICR cell, where they were stored and accumulated over typically 20 laser pulses. Depending on the exact source settings, solvated electrons with up to about 60 water ligands can be produced. The clusters were allowed to interact for a desired length of time with the reactant gas. The neutral reactant acetonitrile-d_3, (99.6%D, Aldrich) was degassed through five freeze−pump−thaw cycles and introduced into the high vacuum via a leak valve, raising the pressure within the instrument to a stable value of typically 9.6×10^{-9} mbar. The concentration of the reactant clusters and of their ionic reaction products was followed by acquiring mass spectra after defined reaction delays. Absolute rate constants are calculated from the number densities of the reactant ion, and collision efficiencies are calculated as the ratio of the absolute rate constant and the collision rate, which in turn was calculated with average dipole orientation (ADO) theory.[33−36]

Density functional calculations were carried out with the Gaussian98 program package,[37] using the BPW91 method with the 6-311++G** basis set. Partial charges were calculated using natural population analysis[38] as implemented in Gaussian98.

Results and Discussion

Reactions of $(H_2O)_n^-$ with CD_3CN. Figure 1a exemplifies a typical initial distribution of clusters taken after a reaction delay of 0 s. In the early stages the reaction proceeds in a manner identical to the normal acetonitrile, that is according to eq 1, except that in this case the neutral, and therefore unobserved, product formed is apparently CD_3CHN. The $OH^-(H_2O)_m$ products do not contain significant amounts of deuterium, and the proposed mechanism is consistent with the absence of isotopic scrambling. Also the fragmentation proceeds in the identical manner and with similar rates, so that after about 10 s all the hydrated electron clusters are replaced by the hydroxide clusters, $OH^-(H_2O)_m$. No exchange of hydrogen against deuterium is observed at this stage.

After about 15 s, as shown in Figure 1b, the first evidence of the incorporation of acetonitrile-d_3 into the hydrated hydroxide clusters is observed:

$$OH^-(H_2O)_m + CD_3CN \rightarrow OH^-(CD_3CN)(H_2O)_{m-x} + xH_2O \quad (2)$$

where probably $x = 1$. The $OH^-(CD_3CN)(H_2O)_p$ product cluster sizes after 15 s range from $p = 4$ to $p = 10$, with the $p = 7$ cluster standing out, having about a factor of 2 higher intensity than the neighboring $p = 6$ and $p = 8$ species. Apparently, for larger clusters reaction 2 does not take place, but as the clusters lose water, it becomes progressively more favorable.

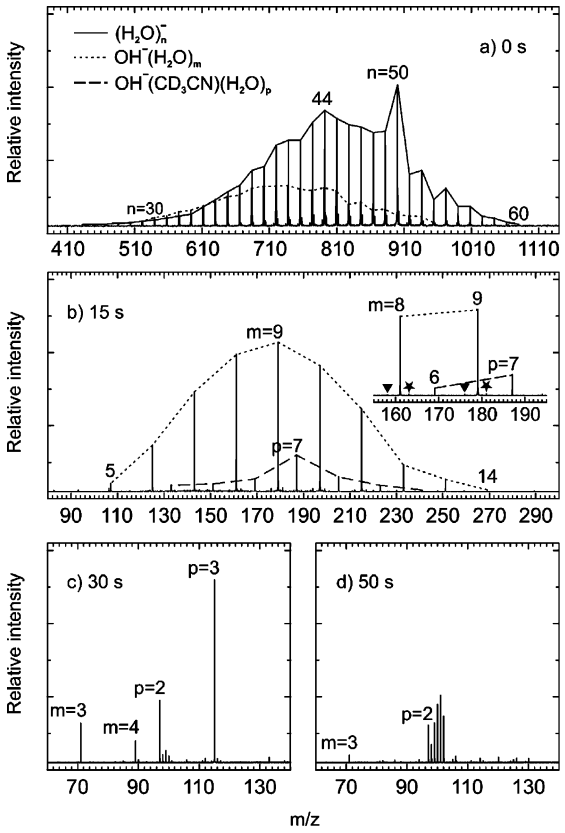

Figure 1. Mass spectra of the reaction of $(H_2O)_n^-$ with acetonitrile-d_3. (a) Since the reaction occurs already during the ion accumulation, the $OH^-(H_2O)_m$ products, shifted by 1 amu to the left, are visible already at 0 s. (b) After 15 s the reaction products have become basic enough that the intake of one acetonitrile-d_3 molecule is possible. In the detail one can see that alongside $OH^-(H_2O)_{8,9}$ growing $OH^-(CD_3CN)(H_2O)_{6,7}$ peaks are visible. Species ▼ $O_2^-(H_2O)_p$ are present due to minor impurities of O_2 in the expansion gas, ★ denotes peaks due to the natural abundance of ^{18}O in $OH^-(H_2O)_m$. (c) The ions gradually lose ligands until after 30 s the main products are $OH^-(H_2O)_{3,4}$, $OH^-(CD_3CN)(H_2O)_2$, and $OH^-(CD_3CN)(H_2O)_3$. The peaks at 98, 99, 100, 101, and 102 amu are due to the progresive deuteration of the $OH^-(CD_3CN)(H_2O)_2$ cluster through a reversible intracluster proton-transfer reaction followed by an acetonitrile ligand exchange. (d) The H/D isotopic exchange reaction proceeds until all the hydrogen atoms are replaced by deuterium.

The latest stages of the reaction are shown in Figure 1, panels c and d, which show spectra obtained after 30 and 50 s, respectively. In the 30 s spectrum, the most intense clusters correspond to $p = 3$, $p = 2$, $m = 3$, and $m = 4$ in that order. On the high mass side of the $p = 2$, that is $OH^-(CD_3CN)(H_2O)_2$ cluster at a nominal mass of 97 amu, one can clearly observe weak peaks appearing at masses 98, 99, and 100 amu, respectively. After an additional 10 s, the 97 amu peak does become the strongest peak in the spectrum, and its higher mass satellites at 98−100 amu have gained considerably in intensity, with peaks also at 101 and 102 amu now being clearly observable. Finally, in Figure 1d, corresponding to 50 s reaction time, the intensities shift further in favor of the higher masses, so that the 99−102 amu peaks are now more intense than the original 97 amu cluster.

Two conclusions may be drawn from these data: The ligand exchange reaction 2 proceeds rather reluctantly, which suggests it might be thermoneutral or slightly endothermic. During further collisions with the CD_3CN molecules, the $OH^-(CD_3CN)(H_2O)_2$ cluster is being progressively deuterated.

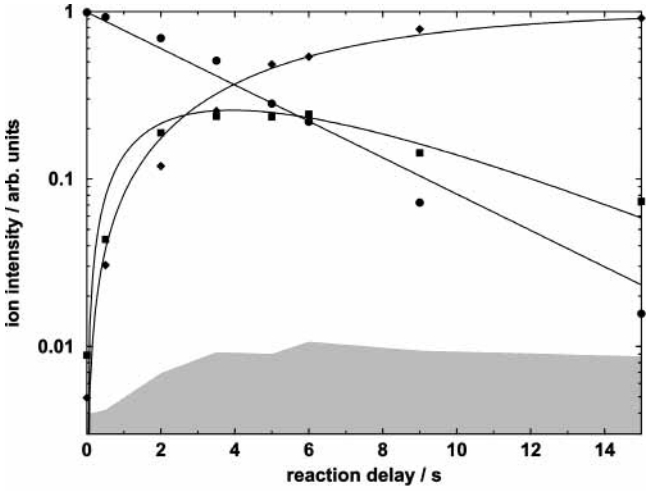

Figure 2. Kinetic fit of mass selected ● $OH^-(CD_3CN)(H_2O)_3$, which loses CD_3CN with a rate constant of $k = 0.18\ s^{-1}$ to form ■ $OH^-(H_2O)_3$ and H_2O with a rate constant of $k = 0.07\ s^{-1}$ to form ◆ $OH^-(CD_3CN)(H_2O)_2$. These fragmentations are induced by blackbody radiation as well as collisions, making them essentially a unimolecular reaction. $OH^-(H_2O)_3$ undergoes a ligand exchange to form $OH^-(CD_3CN)(H_2O)_2$ with $k = 0.26\ s^{-1}$, which amounts to a bimolecular rate constant of $1.1 \times 10^{-9}\ cm^3\ s^{-1}$ or 40% collision efficiency.[33−35] The intensity of subsequent H/D-exchange products was summed into that of $OH^-(CD_3CN)(H_2O)_2$. The gray shaded area denotes the noise level.

Uptake of CD_3CN by $OH^-(H_2O)_n$. To learn more about these processes, we mass selected the $m/z = 115-117$ species after 30 s, i.e., $OH^-(CD_3CN)(H_2O)_3$ including the ^{13}C, ^{18}O isotope peaks and monitored its further reaction for additional 15 s. The time−intensity profile of this reaction is shown in Figure 2, together with a fit according to pseudo-first-order kinetics. It is unambiguously shown that both CD_3CN and H_2O can be lost from the cluster, with a branching ratio of 0.72:0.28. In view of the higher number of H_2O molecules present in the cluster, this clearly indicates that CD_3CN is more weakly bound than H_2O, and that the ligand exchange reaction 2 is in fact slightly endothermic. In addition, the absence of peaks with $m/z = 72-78$, corresponding to partially deuterated $OH^-(H_2O)_3$, is clear evidence that no isotopic scrambling takes place in $OH^-(CD_3CN)(H_2O)_3$. The $OH^-(H_2O)_3$ fragment in turn undergoes the ligand exchange reaction 2, forming $OH^-(CD_3CN)(H_2O)_2$, which do not fragment any further. The product $OH^-(CD_3CN)(H_2O)_2$ can thus be formed in two ways: As a primary product by water loss from $OH^-(CD_3CN)(H_2O)_3$, or as a secondary product by ligand exchange of $OH^-(H_2O)_3$ with CD_3CN.

These results suggest that the ligand exchange reaction 2 is in fact endothermic over the whole region where it occurs, and the CD_3CN are lost again with a high probability due to blackbody radiation and collision-induced dissociation. This explains why the ligand exchange products do not become the dominant species for a very long time and why their intensities exhibit a fairly gradual onset around $n = 10-11$. We have shown previously[39] that aqueous clusters containing OH^- can be viewed as strongly basic. Conversely, acetonitrile is known to be a very weak acid. As the number of water ligands decreases, the basicity of $OH^-(H_2O)_n$ increases, until it is sufficient to make incorporation of CH_3CN into the cluster energetically feasible.

H/D-Exchange in $OH^-(CD_3CN)(H_2O)_2$. Returning to the H/D-exchange, the results so far indicate that only the "final" $OH^-(CD_3CN)(H_2O)_2$ clusters are being efficiently deuterated.

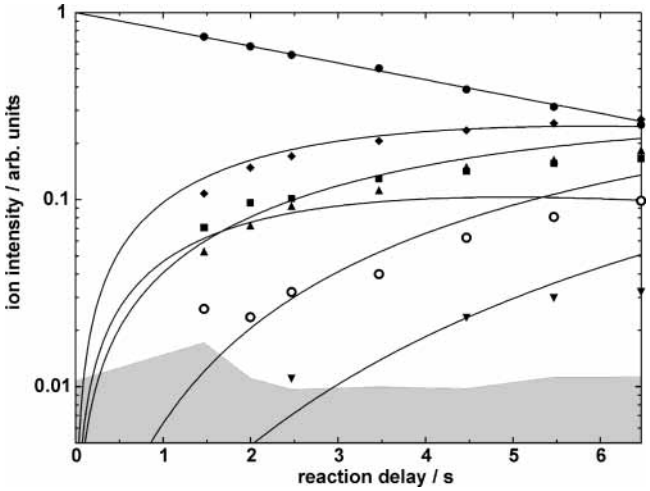

Figure 3. Kinetic fit for the progressive deuteration of mass selected ● $OH^-(CD_3CN)(H_2O)_2$. The symbols denote the number of additional exchanges of H against D: ■ one, ◆ two, ▲ three, ○ four, and ▼ five, the latter corresponding to the completely deuterated final product $OD^-(CD_3CN)(D_2O)_2$. Since the H/D-exchange products overlap with other isotopes such as ^{13}C and ^{18}O, the intensities were corrected for these contributions.

We now performed a mass selection of the 97−102 amu region of the mass spectrum after 35 s by resonant ejection of all ions outside this mass range and followed the gradual deuteration of the $OH^-(CD_3CN)(H_2O)_2$ for an additional 5 s. The time-intensity profile of the results of this experiment is shown in Figure 3, where the intensities of the higher masses have been corrected for the ^{13}C, ^{16}N, and ^{18}O contributions from lower-mass peaks.

It is immediately interesting to note that the ion which grows in first and fastest is not 98 amu, but 99 amu, corresponding to exchange of two hydrogen atoms for deuterium. To rationalize this process, one has to assume that a reversible intracluster reaction is taking place, which exchanges protons between the "organic" part, that is the CD_3CN, and the "aqueous" part, that is the $OH^-(H_2O)_2$. The initial step is described by reaction 3, which redistributes a proton and a deuteron between the two parts:

$$\begin{aligned} OH^-\cdots CD_3CN(H_2O)_2 &\rightarrow HOD\cdots CD_2CN^-(H_2O)_2 \rightarrow \\ &HOH\cdots CD_2CN^-(H_2O)(HOD) \rightarrow \\ &OH^-\cdots CD_2HCN(H_2O)(HOD) \quad (3) \end{aligned}$$

On the time scale of the ICR experiment of seconds, the cluster has enough time to undergo multiple intracluster H/D-exchanges of this type, which will essentially randomize the position of hydrogen and deuterium atoms, modified only by the different zero-point energies of the various isomers.

In a subsequent two-body collision with acetonitrile-d_3, the isotopically scrambled $CD_{3-k}H_kCN$ may be replaced with a fully deuterated CD_3CN according to reaction 4:

$$\begin{aligned} H_{5-k}D_kO_3^-\cdots CD_{3-k}H_kCN + CD_3CN &\rightarrow \\ H_{5-k}D_kO_3^-\cdots CD_3CN + CD_{3-k}H_kCN,\ k = 0-3 \quad (4) \end{aligned}$$

The products of reaction 4 may in turn randomize the position of H and D in reaction similar to reaction 3. In this way, full deuteration is gradually achieved.

If this picture is correct, the time−intensity profile shown in Figure 3 depends only on two factors: The rate with which the

TABLE 1: Pseudo-First-Order Rate Constants k_{exp} for H/D-Exchange Processes of $OH^-(CD_3CN)(H_2O)_2$ in Binary Collisions with CD_3CN from the Fit Shown in Figure 3

j,*k*	k_{exp}	k_{rand}[a]	$p_j(k)$[a]
5,1	0.062	0.059	15/56
5,2	0.118	0.118	30/56
5,3	0.038	0.039	10/56
4,1	0.035	0.094	24/56
4,2	0.035	0.094	24/56
4,3	0.005	0.016	4/56
3,1	0.085	0.118	30/56
3,2	0.040	0.059	15/56
3,3	0.003	0.004	1/56
2,1	0.095	0.118	30/56
2,2	0.020	0.024	6/56
1,1	0.080	0.083	21/56

[a] The reactions describe the exchange of *k* H against D in a cluster containing *j* H. Theoretical numbers k_{rand} based on the assumption of total randomization in the cluster and a constant exchange rate of the acetonitrile molecule, as well as their statistical contribution $p_j(k)$, are shown for comparison.

$CD_{3-k}H_kCN$ is exchanged against CD_3CN, and the probability $p_j(k)$ for a certain value of *k* in a cluster containing *j* H atoms and 8-*j* D atoms. This probability can be calculated with a standard equation from combinatorial mathematics and amounts to:

$$p_j(k) = \frac{\binom{j}{k}\binom{8-j}{3-k}}{\binom{8}{3}} \qquad (5)$$

In the first exchange step, $j = 5$, and the probabilities for exchanging 0, 1, 2, or 3 D against H, i.e., $k = 0$, 1, 2, or 3, are 1/56, 15/56, 30/56, and 10/56, respectively. A fit of the decay of the reactant $m/z = 97$ yields a relative rate constant of $k_{rel} = 0.21\ s^{-1}$. The total exchange rate constant on which the complete fit must be based is then 56/55 $k_{rel} = 0.22\ s^{-1}$, which corresponds to an absolute rate constant for the exchange of $k_{abs} = 9.4 \times 10^{-10}\ cm^3\ s^{-1}$ or a collision efficiency of $\Phi =$ 36%. Table 1 compares the ideal rate constants calculated from these assumptions with the actual rate constants extracted from the fit. The rate constants for primary products are very well reproduced by this approach, especially the observation that the probability for exchanging two H atoms in the first step is twice as high as for one H. The subsequent exchange steps, however, exhibit substantial deviations from this ideal picture, although the overall pattern is still well reproduced. In this simple approach, the energy differences due to the variations of vibrational frequencies with the position of H and D is neglected, which changes the relative probabilities as well as the rate constant for the exchange.

A second possibility is that scrambling may also occur to some extent in the collision complex, while full randomization in the collision complex can be excluded: The probability for exchange of one or two H atoms in the first step would be 5/11 or 4/11, respectively, while the data clearly indicate that exchange of two H atoms against D is preferred by a factor of 2. Given the simplicity of the approach, the agreement of the fit is quite remarkable and indicates that the overall picture of the H/D-exchange process is correct.

The observed H/D-exchange also is indirect evidence that no base-catalyzed hydrolysis of acetonitrile to acetic acid takes place in these small gas phase clusters, which occurs under strongly basic conditions in aqueous solutions. However, the mechanism of this hydrolysis is very complicated

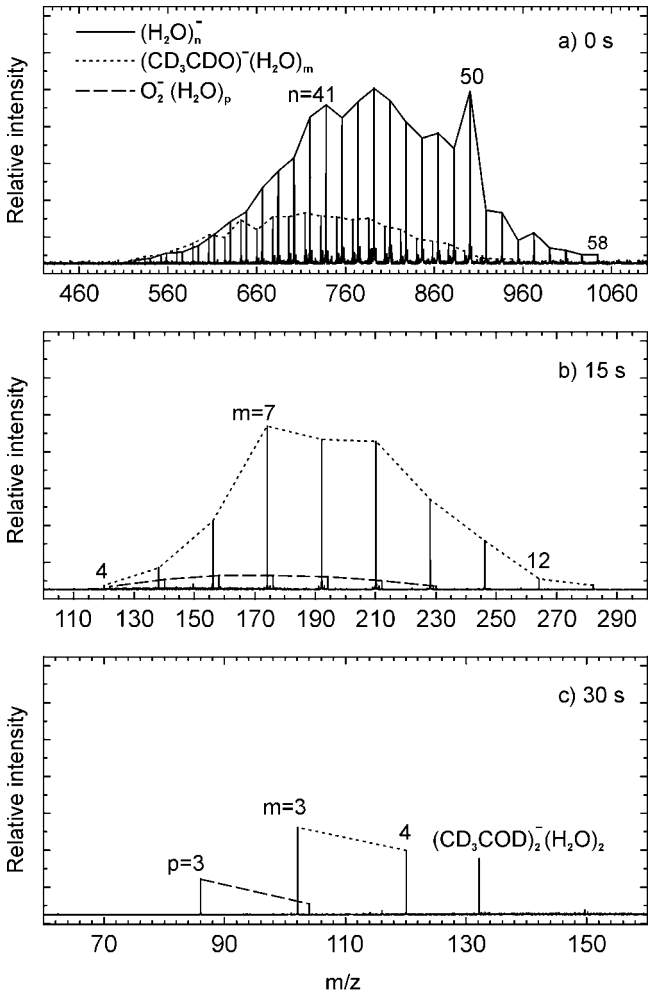

Figure 4. Mass spectra of the reaction of $(H_2O)_n^-$ with perdeuterated acetaldehyde. (a) One CD_3CDO molecule is taken up by the hydrated electron clusters as can be seen already at nominally 0 s. (b) The exchange is complete and fragmentation in full progress at 15 s. (c) After 30 s the main products are $CD_3CDO^-(H_2O)_{3,4}$, $(CD_3CDO)_2^-(H_2O)_2$, and $O_2^-(H_2O)_3$ as impurity. No H/D exchange peaks are visible, which supports the role of the hydroxide anion in the suggested exchange mechanism.

and involves multiple proton-transfer steps. If CD_3COO^- would form, the $m = 2$ product would have the composition $CD_3COO^-(NH_3)(H_2O)$, if scrambling is neglected. Under these conditions, replacement of a CD_3CN unit seems highly improbable.

Reactions of $(H_2O)_n^-$ with CD_3CDO. To provide additional evidence that the presence of the hydroxide anion and the basicity of the cluster are responsible for the H/D-exchange, we have carried out a similar experiment with perdeuterated acetaldehyde, CD_3CDO, instead of acetonitrile, as shown in Figure 4. The polar CD_3CDO is efficiently taken up by the hydrated electron clusters, and solvated $CD_3CDO^-(H_2O)_m$ anions are formed. Similar to other cases, like O_2 or CO_2 reactions,[21,22] where the exchange of the ligand is accompanied by a change in the nature of the central ion, after a single molecule of the reactant has entered the cluster, no further uptake of acetaldehyde is observed for larger clusters. The clusters then only fragment and progressively lose ligands one by one, down to $m = 3$. However, when the clusters become very small, again an endothermic ligand exchange becomes feasible, and more and more $(CD_3CDO)_2^-(H_2O)_2$ is observed. Even after 30 s, however, no H/D-exchange peaks are detectable in these clusters, where no OH^- anions are present. After 50 s, the signal

TABLE 2: Relative Energy (kJ/mol) of $OH^-(CH_3CN)(H_2O)_m$ (Structure A) and $(CH_2CN^-)(H_2O)_{m+1}$ (Structure B), Dissociation Energy (kJ/mol) of the Most Stable Isomer for Each Size, and Natural Population Analysis (atomic unit) of Selected Fragments[a]

	$OH^-(CH_3CN)(H_2O)_m$ (A) $CH_2CN^-(H_2O)_{m+1}$ (B)	relative energy	dissociation energy		total fragment charge from natural population analysis[38]				
			$-CH_3CN$	$-H_2O$	CH_3CN	$OH^-(H_2O)_m$	OH^-	CH_2CN^-	$(H_2O)_{m+1}$
$m=0$	B_{0-1}	0.0						−0.88	−0.12
$m=1$	A_{1-1}	0.0	72.6	53.9	−0.13	−0.87	−0.75		
	B_{1-1}	8.4						−0.85	−0.15
$m=2$	A_{2-1}	0.0	58.1	64.2	−0.07	−0.93	−0.75		
	A_{2-2}	3.1			−0.04	−0.96	−0.73		
	B_{2-1}	31.0						−0.84	−0.16
	B_{2-2}	31.2						−0.83	−0.17
$m=3$	A_{3-1}	6.0			−0.06	−0.94	−0.73		
	A_{3-2}	0.0	48.4	54.1	−0.03	−0.97	−0.73		
	B_{3-1}	51.2						−0.83	−0.17
	B_{3-2}	47.0						−0.83	−0.17

[a] The energies are evaluated by the BPW91/6-311++G** method with zero point energy correction.

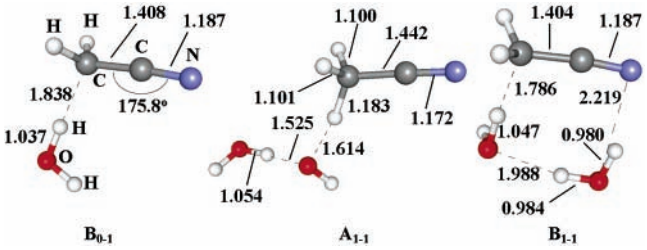

Figure 5. Optimized geometries for the isomers $OH^-CH_3CN(H_2O)_m$ (Structure A) and $CH_2CN^-(H_2O)_{m+1}$ (Structure B), for $m = 0$ and 1. The strong interaction between OH^- and CH_3CN with a short CH···OH distance (1.614 Å) in A_{1-1} suggests a low barrier for the proton transfer from CH_3CN to OH^-.

has disappeared due to slow, presumably collision-induced electron detachment.

The total absence of H/D-exchange peaks in $CD_3CDO^-(H_2O)_3$ after 30 s, when the exchange was in full progress in $OH^-CD_3CN(H_2O)_2$, provides additional strong evidence that the H/D-exchange mechanism requires the hydroxide anion, as suggested in reaction 3.

Density Functional Calculations of $OH^-(CH_3CN)(H_2O)_m$, $m = 0-3$. We have further checked the feasibility of the H/D-exchange mechanism suggested by reactions 3 and 4 by a series of quantum chemical calculations on the $OH^-(CH_3CN)(H_2O)_m$, $m = 0-3$ clusters. Consistent with the proposed proton transfer, we find for most of the clusters two types of structures: $OH^-(CH_3CN)(H_2O)_m$ solvated hydroxide complexes which we denote in Table 2 and Figures 5−8 with the letter A_{m-i}, and complexes $(CH_2CN^-)(H_2O)_{m+1}$ denoted B_{m-i}. In the latter, the acetonitrile has transferred one proton to OH^-, yielding a molecule of water and resulting in a solvated CH_2CN^- anion. Obviously, the relative energies of these isomeric forms, and the barriers separating them, are crucial for the proposed proton transfer and isotope exchange processes. To distinguish different isomers of the same A_m, B_m species, a second index i is introduced. The results are summarized in Table 2, which lists relative energies and the partitioning of the negative charge over the hydrogen bonded species in the cluster, according to natural population analysis.[38] The energetically lowest lying isomers of A_m and B_m for $m = 0-3$ are shown in Figures 5−7.

A complex of OH^- with CH_3CN, which would in this notation be A_{0-1}, is found not to be stable; as soon as a hydroxide anion comes into contact with acetonitrile, a proton transfer takes place, resulting in the CH_2CN^- anion bound to a water ligand (B_{0-1} in Figure 5). The H_2O is bonded via a rather long, 1.838 Å hydrogen bond to the carbon atom of the CH_2-group, which carries a formal charge of −0.97e. The CCN bond angle with 175.8° deviates only slightly from linearity, and there is only little charge transfer from the CH_2CN^- to the water ligand, with the electron residing mostly on the organic anion (−0.88e).

Already a single additional water molecule stabilizes the OH^- anion, so that both kinds of structures represent local minima on the potential energy surface. The A_{1-1} complex (Figure 5) is a structure of $OH^-(CH_3CN)(H_2O)$ in which the OH^- is stabilized by two ligands, one molecule of water and acetonitrile. In this complex, acetonitrile binds to the OH^- via one of the hydrogen atoms of the methyl group. The hydrogen-bonded C−H is appreciably lengthened to 1.183 Å, and the hydrogen bonding distance (1.614 Å) is remarkably short, comparable to the hydrogen bonding distance between the OH^- and H_2O (1.525 Å). A charge of −0.75e is computed to be localized on the OH^-, with −0.12e and −0.13e on the water ligand and on the acetonitrile, respectively. The proton transferred structure $(CH_2CN^-)(H_2O)_2$ (B_{1-1} in Figure 5) is also a stable local minimum, with energy of only 8.4 kJ/mol higher than that of A_{1-1}. The negative charge again largely resides on the organic anion (−0.85e). The CH_2CN^- anion is bound to a water dimer by two hydrogen bonds with C···H and N···H distances of 1.786 Å and 2.219 Å, respectively.

Additional water ligands then further stabilize the hydroxide anion, reducing its basicity, and this is also reflected in the corresponding cluster structures, which are reproduced in Figures 6 and 7. The strength of the OH^-−acetonitrile hydrogen bond is reduced, and this is clearly evidenced by the H···O distance increasing with the added ligands from the unusually short value of 1.614 Å in A_{1-1} to 1.812 and 1.841 Å in A_{2-1} and A_{3-1}, respectively. Concurrently, the C−H bond length, which is with 1.183 Å unusually long in A_{1-1}, exhibits progressively less lengthening in the larger species. Clearly, the lengthened hydrogen bond and shortened C−H bond will make proton transfer and isotopic exchange in the larger clusters much less favorable. The increased stability of the hydroxide anion is also reflected by a higher negative charge remaining on the $OH^-(H_2O)_m$ cluster, and correspondingly less transfer onto the acetonitrile molecule (Table 1). Obviously, with increasing number of water ligands, more local minima and isomers become possible, and this is exemplified in Table 1 and Figures 6 and 7 by the structures A_{2-2}, B_{2-2}, A_{3-2} and B_{3-2}.

The increasing stabilization of the OH^- anion also has the consequence that with the number of water ligands the alternative, proton-transferred structures become energetically less favorable, as may clearly be seen in Table 1. While the $m = 1$ species are close to isoenergetic, with B_{1-1} being computed only 8.4 kJ/mol above A_{1-1}, the difference increases steeply to around 30 kJ/mol for $m = 2$ and almost 50 kJ/mol for $m = 3$. The

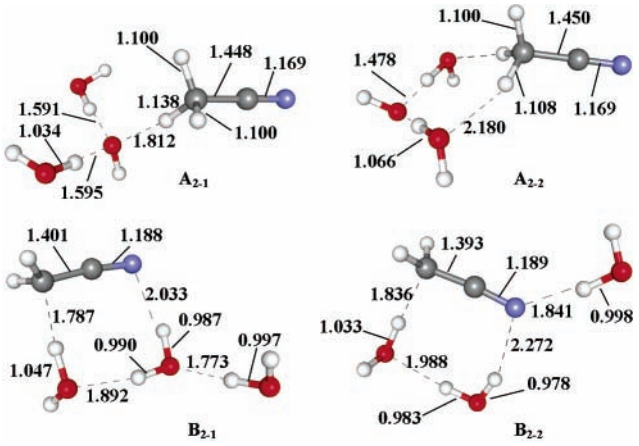

Figure 6. Optimized geometries for the isomers $OH^-CH_3CN(H_2O)_m$ (Structure A) and $CH_2CN^-(H_2O)_{m+1}$ (Structure B), for $m = 2$. Structures A_{m-2} are characterized by two hydrogen bonds from the methyl group to water molecules, with the OH^- ion moved to a more remote position. B_{m-2} structures feature two water molecules hydrogen bonded to the nitrile group.

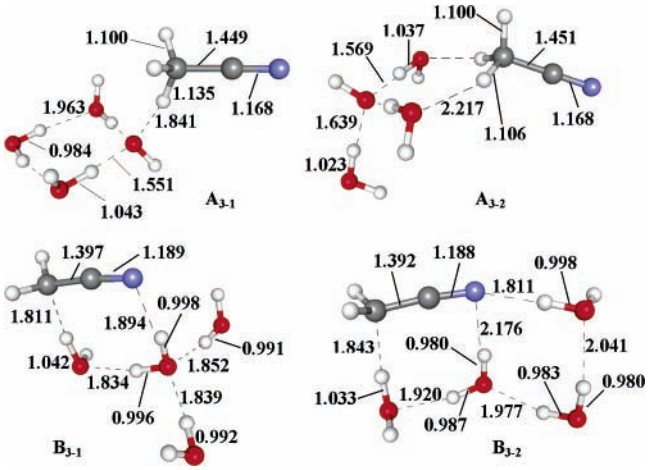

Figure 7. Optimized geometries for the isomers $OH^-CH_3CN(H_2O)_m$ (Structures A) and $CH_2CN^-(H_2O)_{m+1}$ (Structures B), for $m = 3$. The lower energy structures are here A_{3-2} and B_{3-2}, the difference albeit being small. However, in A_{3-2} the OH^- does not directly attack the methyl group, and at the same time, no H/D-exchange is observed for the $m = 3$ clusters.

computed isomers are still close enough in energy to be thermally accessible on the time scale of the ICR experiment, at least for $m = 2$ and 3. The H/D-exchange process is, however, observed only for $m = 2$. Actually, no clusters with only two ligands, that is either $OH^-(H_2O)_2$ or $OH^-(CH_3CN)(H_2O)$, are detected in our experiments. This is consistent with the relatively high 58.1 and 64.2 kJ/mol computed dissociation energies of the $OH^-(CH_3CN)(H_2O)_2$ cluster to lose CH_3CN and H_2O, respectively (Table 1). For the next larger cluster, $OH^-(CH_3CN)(H_2O)_3$, the dissociation energies to generate $OH^-(H_2O)_3$ and $OH^-(CH_3CN)(H_2O)_2$ are 48.4 and 54.1 kJ/mol, respectively. This is thus approximately the maximum amount of energy a cluster anion of this size can absorb in the ICR chamber without falling apart. This energy is considerably higher than the about 30 kJ/mol difference between $OH^-(CH_3CN)(H_2O)_m$ and $(CH_2CN^-)(H_2O)_{m+1}$ for $m = 2$, the cluster size for which we observe the efficient H/D-exchange process. However, already for $m = 3$ the energy difference between $OH^-(CH_3CN)(H_2O)_m$ and $(CH_2CN^-)(H_2O)_{m+1}$ is comparable to the energy required for cluster dissociation. As a consequence, for larger clusters,

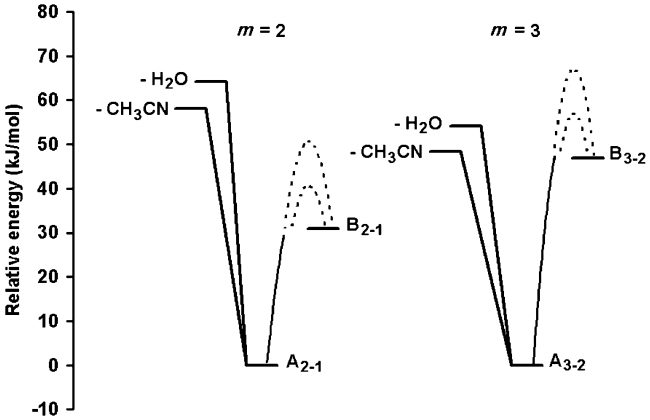

Figure 8. Potential energy surface of the H/D-exchange reaction for $m = 2$ and $m = 3$. For H/D-exchange to occur, an isomer of type A has to be converted to B and back. For $m = 3$, loss of CH_3CN or H_2O is energetically more favorable than conversion from A_{3-2} to B_{3-2}, while for $m = 2$, the situation is reversed. Consequently, H/D-exchange is only observed for $m = 2$. The dotted lines give a conservative lower and upper estimate for the barrier separating the isomers, which is described in detail in the text.

such irreversible dissociation process should become dominant, and accordingly, no H/D-exchange is detected for $m > 2$.

Figure 8 illustrates the potential energy surface of the relevant species, comparing ligand loss with isotopic scrambling. While for $m = 2$ the barrier for interconversion between A_{2-1} and B_{2-1} is readily overcome before ligand loss can occur, the situation is reversed for $m = 3$. Although we have not located the probably multiple transition states of this interconversion reaction, we can assume barriers of 10−20 kJ/mol for the rearrangement of hydrogen bonds in water clusters. The strength of one hydrogen bond of 20 kJ/mol[40] poses a conservative upper limit to the barrier, while a concerted mechanism can probably work with half this value. Since the isomerization from B_{m-1} to A_{m-1} starts with the rearrangement of one hydrogen bond, the ranges shown in the picture for the barriers are believed to be quantitative. The calculations consistently explain why isotopic scrambling is only observed for $m = 2$.

Conclusions

Hydrated electrons $(H_2O)_n^-$ are in collisions with acetonitrile-d_3 efficiently converted to hydrated hydroxide, $OH^-(H_2O)_m$ clusters, without isotopic scrambling. As the large clusters fragment and lose ligands, they become increasingly basic, so that when about $m = 10-12$ is reached, they are able take up an acetonitrile molecule. The fragmentation process continues with a parallel loss of acetonitrile-d_3 and water and uptake of acetonitrile-d_3 by ligand exchange, until $OH^-(CD_3CN)(H_2O)_2$ are formed. These species exhibit an interesting H/D isotopic exchange reaction, in which they are progressively deuterated in collisions with gaseous CD_3CN. This deuteration is due to repeated proton transfers and isomerizations within the $OH^-(CD_3CN)(H_2O)_2$ cluster, followed by ligand exchange, in which a partially deuterated $CD_{3-k}H_kCN$ is replaced by CD_3CN. This reaction proceeds until all the H atoms are replaced by deuterium, forming the final product $OD^-(CD_3CN)(D_2O)_2$. To find further support for the role of OH^- and of the basicity of the clusters, similar experiments were carried out with fully deuterated acetaldehyde. This is efficiently taken up by the cluster in the first reaction step, without formation of a hydroxide anion. Consequently, no trace of H/D-exchange is observed throughout the reaction. Density functional calculations map stationary points on the potential energy surface of the H/D-

exchange reaction. The calculated energetics explain why H/D-exchange occurs only in the smallest cluster observed.

Acknowledgment. We thank European Union through the Research Training Network "Reactive Intermediates Relevant in Atmospheric Chemistry and Combustion", the Deutsche Forschungsgemeinschaft, the Fonds der Chemischen Industrie, and the Alexander von Humboldt-Foundation (C.-K.S.) for financial support.

Supporting Information Available: Optimized geometries, natural population analyses, and thermochemistry output of the structures shown in Figures 5, 6, and 7. This material is available free of charge via the Internet at http://pubs.acs.org.

References and Notes

(1) Campbell, S.; Rodgers, M. T.; Marzluff, E. M.; Beauchamp, J. L. *J. Am. Chem. Soc.* **1994**, *116*, 9765.
(2) Cassady, C. J.; Carr, S. R. *J. Mass Spectrom.* **1996**, *31*, 247.
(3) Cheng, X. H.; Fenselau, C. *Int. J. Mass Spectrom. Ion Processes* **1992**, *122*, 109.
(4) Freitas, M. A.; Marshall, A. G. *Int. J. Mass Spectrom.* **1999**, *183*, 221.
(5) Green, M. K.; Lebrilla, C. B. *Mass Spectrom. Rev.* **1997**, *16*, 53.
(6) Gur, E. H.; Dekoning, L. J.; Nibbering, N. M. M. *J. Am. Soc. Mass Spectrom.* **1995**, *6*, 466.
(7) Koster, G.; Lifshitz, C. *Int. J. Mass Spectrom.* **1999**, *183*, 213.
(8) Suckau, D.; Shi, Y.; Beu, S. C.; Senko, M. W.; Quinn, J. P.; Wampler, F. M.; McLafferty, F. W. *Proc. Natl. Acad. Sci. U.S.A.* **1993**, *90*, 790.
(9) Winger, B. E.; Lightwahl, K. J.; Rockwood, A. L.; Smith, R. D. *J. Am. Chem. Soc.* **1992**, *114*, 5897.
(10) Wyttenbach, T.; Paizs, B.; Barran, P.; Breci, L.; Liu, D. F.; Suhai, S.; Wysocki, V. H.; Bowers, M. T. *J. Am. Chem. Soc.* **2003**, *125*, 13768.
(11) DePuy, C. H. *Int. J. Mass Spectrom.* **2000**, *200*, 79.
(12) Stewart, J. H.; Shapiro, R. H.; Depuy, C. H.; Bierbaum, V. M. *J. Am. Chem. Soc.* **1977**, *99*, 7650.
(13) Marcus, R. A. *Rev. Mod. Phys.* **1993**, *65*, 599.
(14) Anbar, M. *Adv. Phys. Org. Chem.* **1969**, *7*, 115.
(15) Schindewolf, U. *Angew. Chem., Int. Ed.* **1968**, *7*, 190.
(16) Anderson, P. A.; Barr, D.; Edwards, P. P. *Angew. Chem., Int. Ed. Engl.* **1991**, *30*, 1501.
(17) Verma, N. C.; Fessenden, R. W. *J. Chem. Phys.* **1976**, *65*, 2139.
(18) Buxton, G. V.; Greenstock, C. L.; Helman, W. P.; Ross, A. B. *J. Phys. Chem. Ref. Data* **1988**, *17*, 513.
(19) Coe, J. V.; Lee, G. H.; Eaton, J. G.; Arnold, S. T.; Sarkas, H. W.; Bowen, K. H.; Ludewigt, C.; Haberland, H.; Worsnop, D. R. *J. Chem. Phys.* **1990**, *92*, 3980.
(20) Ayotte, P.; Johnson, M. A. *J. Chem. Phys.* **1997**, *106*, 811.
(21) Posey, L. A.; Deluca, M. J.; Campagnola, P. J.; Johnson, M. A. *J. Phys. Chem.* **1989**, *93*, 1178.
(22) Arnold, S. T.; Morris, R. A.; Viggiano, A. A.; Johnson, M. A. *J. Phys. Chem.* **1996**, *100*, 2900.
(23) Bondybey, V. E.; Beyer, M. K. *Int. Rev. Phys. Chem.* **2002**, *21*, 277.
(24) Beyer, M. K.; Fox, B. S.; Reinhard, B. M.; Bondybey, V. E. *J. Chem. Phys.* **2001**, *115*, 9288.
(25) Balaj, O. P.; Balteanu, I.; Fox-Beyer, B. S.; Beyer, M. K.; Bondybey, V. E. *Angew. Chem., Int. Ed.* **2003**, *42*, 5516.
(26) Shkrob, I. A.; Sauer, M. C. *J. Phys. Chem. A* **2002**, *106*, 9120.
(27) Shkrob, I. A.; Takeda, K.; Williams, F. *J. Phys. Chem. A* **2002**, *106*, 9132.
(28) Xia, C. G.; Peon, J.; Kohler, B. *J. Chem. Phys.* **2002**, *117*, 8855.
(29) Berg, C.; Schindler, T.; Niedner-Schatteburg, G.; Bondybey, V. E. *J. Chem. Phys.* **1995**, *102*, 4870.
(30) Bondybey, V. E.; English, J. H. *J. Chem. Phys.* **1981**, *74*, 6978.
(31) Dietz, T. G.; Duncan, M. A.; Powers, D. E.; Smalley, R. E. *J. Chem. Phys.* **1981**, *74*, 6511.
(32) Fox, B. S.; Balaj, O. P.; Balteanu, L.; Beyer, M. K.; Bondybey, V. E. *Chem. Eur. J.* **2002**, *8*, 5534.
(33) Bass, L.; Su, T.; Bowers, M. T. *Int. J. Mass Spectrom. Ion Processes* **1978**, *28*, 389.
(34) Bass, L.; Su, T.; Chesnavich, W. J.; Bowers, M. T. *Chem. Phys. Lett.* **1975**, *34*, 119.
(35) Su, T.; Bowers, M. T. *J. Chem. Phys.* **1973**, *58*, 3027.
(36) Beyer, M. K.; Berg, C. B.; Bondybey, V. E. *Phys. Chem. Chem. Phys.* **2001**, *3*, 1840.
(37) Frisch, M. J.; Trucks, G. W.; Schlegel, H. B.; Scuseria, G. E.; Robb, M. A.; Cheeseman, J. R.; Zakrzewski, V. G.; Montgomery, J. A., Jr.; Stratmann, R. E.; Burant, J. C.; Dapprich, S.; Millam, J. M.; Daniels, A. D.; Kudin, K. N.; Strain, M. C.; Farkas, O.; Tomasi, J.; Barone, V.; Cossi, M.; Cammi, R.; Mennucci, B.; Pomelli, C.; Adamo, C.; Clifford, S.; Ochterski, J.; Petersson, G. A.; Ayala, P. Y.; Cui, Q.; Morokuma, K.; Malick, D. K.; Rabuck, A. D.; Raghavachari, K.; Foresman, J. B.; Cioslowski, J.; Ortiz, J. V.; Stefanov, B. B.; Liu, G.; Liashenko, A.; Piskorz, P.; Komaromi, I.; Gomperts, R.; Martin, R. L.; Fox, D. J.; Keith, T.; Al-Laham, M. A.; Peng, C. Y.; Nanayakkara, A.; Gonzalez, C.; Challacombe, M.; Gill, P. M. W.; Johnson, B. G.; Chen, W.; Wong, M. W.; Andres, J. L.; Head-Gordon, M.; Replogle, E. S.; Pople, J. A. *Gaussian 98*, revision A.11; Gaussian, Inc.: Pittsburgh, PA, 2001.
(38) Reed, A. E.; Curtiss, L. A.; Weinhold, F. *Chem. Rev.* **1988**, *88*, 899.
(39) Achatz, U.; Joos, S.; Berg, C.; Schindler, T.; Beyer, M.; Albert, G.; Niedner-Schatteburg, G.; Bondybey, V. E. *J. Am. Chem. Soc.* **1998**, *120*, 1876.
(40) Kim, J. S.; Lee, J. Y.; Lee, S.; Mhin, B. J.; Kim, K. S. *J. Chem. Phys.* **1995**, *102*, 310.